

# COMMISSIONING OF THE LCLS LINAC\*

H. Loos<sup>†</sup>, R. Akre, A. Brachmann, F.-J. Decker, Y. Ding, D. Dowell, P. Emma, J. Frisch,  
 S. Gilevich, G. Hays, Ph. Hering, Z. Huang, R. Iverson, C. Limborg-Deprey, A. Miahnahri,  
 S. Molloy, H.-D. Nuhn, J. Turner, J. Welch, W. White, J. Wu, SLAC, Menlo Park, CA 94025, USA  
 D. Ratner, Stanford University, Stanford, CA 94305, USA

## Abstract

The Linac Coherent Light Source (LCLS) X-ray free electron laser project is currently under construction at the Stanford Linear Accelerator Center (SLAC). A new injector and upgrades to the existing accelerator were installed in two phases in 2006 and 2007. We report on the commissioning of the injector, the two new bunch compressors at 250 MeV and 4.3 GeV, and transverse and longitudinal beam diagnostics up to the end of the existing linac at 13.6 GeV. The commissioning of the new transfer line from the end of the linac to the undulator is scheduled to start in November 2008 and for the undulator in March 2009 with first light to be expected in July 2009.

## INTRODUCTION

The Linac Coherent Light Source (LCLS) [1] is an X-ray free electron laser project aimed at generating coherent radiation at wavelengths from 15 Å to 1.5 Å using the final third of the existing SLAC 2-mile accelerator to deliver electrons with an energy of up to 13.6 GeV into an undulator with a length of 130 m. The requirements of a small transverse normalized emittance of  $1.2 \mu\text{m}$  and a peak current of 3 kA to achieve saturation within the length of the undulator are met with the addition of a high brightness photo-injector at the 2/3 point in the linac and two subsequent magnetic chicane bunch compressors. The photo-injector and first bunch compressor was constructed in 2006 and commissioned from April to August 2007 [2, 3]. The second bunch compressor was installed in the fall of 2007 and the second phase of commissioning took place from January to August of 2008 [3].

The layout of the LCLS is depicted in Fig. 1, showing the injector oriented at  $35^\circ$  to the main linac, the two bunch compressors, and some of the diagnostics (LTU and undulator not shown). The main design parameters of the LCLS linac and the achieved values are listed in Table 1.

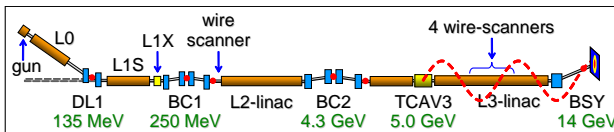


Figure 1: Layout of the LCLS accelerator.

Table 1: LCLS Accelerator Specifications

	Design	Meas.	Unit
Repetition rate	120	30	Hz
Energy	13.6	13.6	GeV
Charge	1	0.25	nC
Bunch length	20	8-10	$\mu\text{m}$
Peak current	3	3	kA
Emittance (injector)	1.2	0.7-1	$\mu\text{m}$
Slice emittance (inj.)	1.0	0.6	$\mu\text{m}$
Emittance (linac end)	1.5	0.7-1.6	$\mu\text{m}$
Laser energy	250	20-150	$\mu\text{J}$
Gun field at cathode	120	115	MV/m
Quantum efficiency	6	0.7-7	$10^{-5}$

Most of the diagnostics for the electron beam were commissioned in the first phase with some additions during the second phase. New beam position monitors in the injector and bunch compressors and upgraded ones in the existing linac achieve between  $5 - 10 \mu\text{m}$  resolution. Images of the beam are obtained with YAG screens in the gun and low energy area of the injector, and OTR foils with up to  $10 \mu\text{m}$  resolution throughout the rest of the machine. Their functioning is presently compromised by the occurrence of coherent optical transition radiation and are expected to become reliable with the installation of a laser heater in the injector, which will suppress coherent effects in the beam. Projected transverse emittance can be measured with OTR screens and wire scanners located in the injector at 135 MeV and after BC1 at 250 MeV with 3-screen or quadrupole scan technique. Four wire scanners halfway in the third linac (L3) at 9 GeV are used to obtain the emittance after the second bunch compressor.

A transverse deflector cavity in the injector and one after BC2 make it possible to measure the longitudinal bunch profile and longitudinal phase space on OTR screens in the injector and a phosphorus screen in a dispersive section downstream of the main linac. The vertically deflecting cavity is also used to obtain the horizontal slice emittance in the injector. A number of phase cavities in the injector and after each bunch compressor give the bunch arrival time. Two relative bunch length monitors after BC1 and BC2 which detect coherent edge radiation from the bunch compressor dipoles provide a non-interceptive signal related to the bunch length. The signals are calibrated against an absolute measurement with the transverse cavity.

\* Work supported by US DOE contract DE-AC02-76SF00515.

<sup>†</sup> loos@slac.stanford.edu

The following sections describe the performance of the drive laser and photo injector, the commissioning of the bunch compressors and the observation of coherent effects of the compressed electron bunch.

## PHOTO-INJECTOR

The drive laser system for the photo-injector uses a regenerative Ti:Sapphire amplifier and frequency tripling to the UV at 255 nm to generate electrons in the copper cathode. With most controls and diagnostics remotely available the laser beam now has an uptime of over 99%.

Profile Monitor CAMR:IN20:186 05-Aug-2008 08:29:58

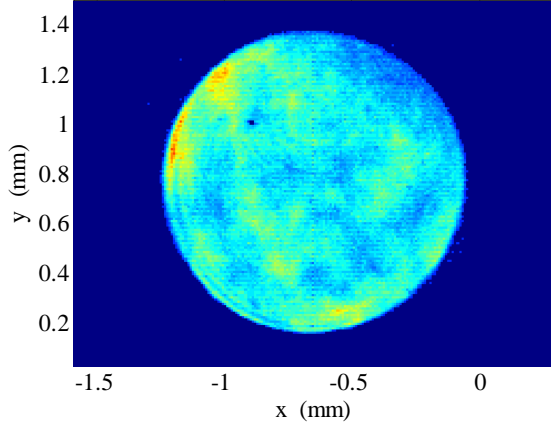


Figure 2: Laser distribution on the virtual cathode.

A typical flat-top transverse distribution of the laser beam on the virtual cathode is shown in Fig. 2 with about 10% rms intensity variation. The UV pulse shape can be seen in Fig. 3, as measured by a cross-correlation with the oscillator pulse. The pulse to pulse rms transverse stability of the laser on the cathode was  $30\text{ }\mu\text{m}$  in the original installation, but could be since be improved to  $10\text{ }\mu\text{m}$  rms by implementing changes to the laser transport line.

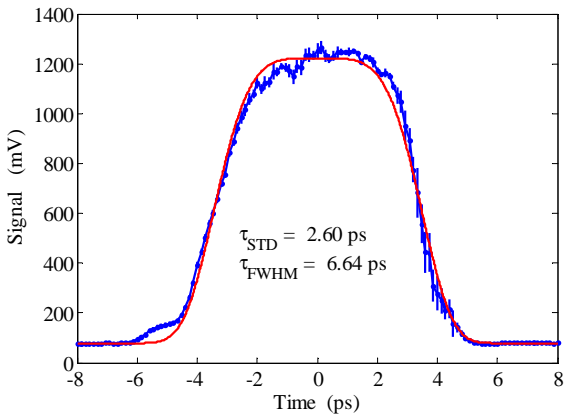


Figure 3: Temporal distribution of the UV-drive laser measured by a cross-correlation with the Ti:Sapphire oscillator.

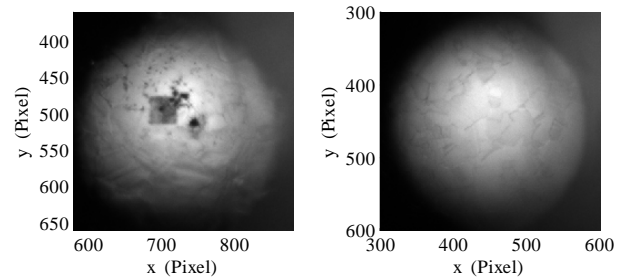


Figure 4: White-light image of the cathode before (left) and after (right) replacement.

While the first year of operation had shown a steady increase of the quantum efficiency (QE) of the copper cathode, it began to steadily drop after a scheduled vacuum break. Initially, a laser cleaning procedure helped to recover the QE, but after repeated cleaning it remained low at  $0.75 \times 10^{-5}$  which limited the bunch charge to  $200\text{ pC}$  at full laser power. The laser cleaning also damaged the cathode surface as can be seen in Fig. 4. The cathode was subsequently replaced and the QE measured to  $7.6 \times 10^{-5}$  as pictured in Fig. 5. The QE is obtained from a linear fit at small laser energy in the range denoted by the dotted line. The charge rolls off at higher laser power due to space charge shielding [4].

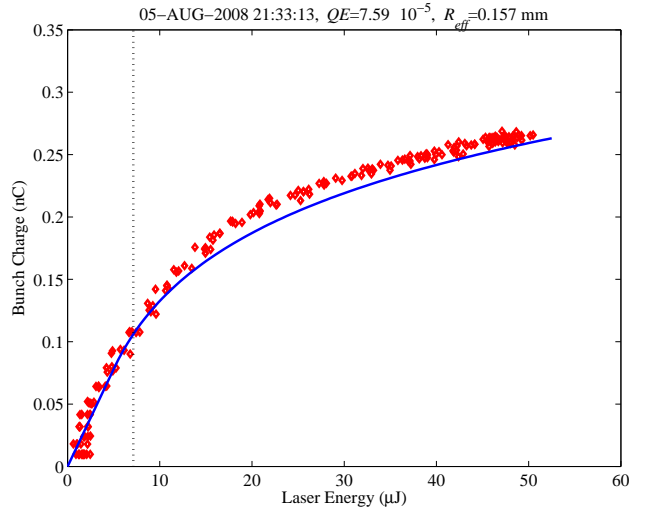


Figure 5: Cathode quantum efficiency obtained from measurement of electron bunch charge vs. laser energy.

The operation of the main linac and the FEL requires stable and repeatable beam parameters from the photo-injector for varying machine configurations such as desired bunch charge and bunch length, as well as for changes in the laser transverse and longitudinal profile and uniformity of the cathode. A procedure has been established to set up the injector magnets to optimize the projected emittance. In an iterative and semi-automated way, the steering or focusing magnet is varied and the projected emittance mea-

sured at each step with a quadrupole scan on an OTR screen downstream of the first two accelerating structures. The magnet is then set to the minimum of the measured emittance. The procedure includes the gun solenoid, a normal and a skew quad embedded within the solenoid, correctors in the gun region to find the optimum trajectory through the first accelerating structure and subsequent matching of the transverse beam phase space to the design Twiss parameters at the OTR screen location with the upstream injector quadrupoles.

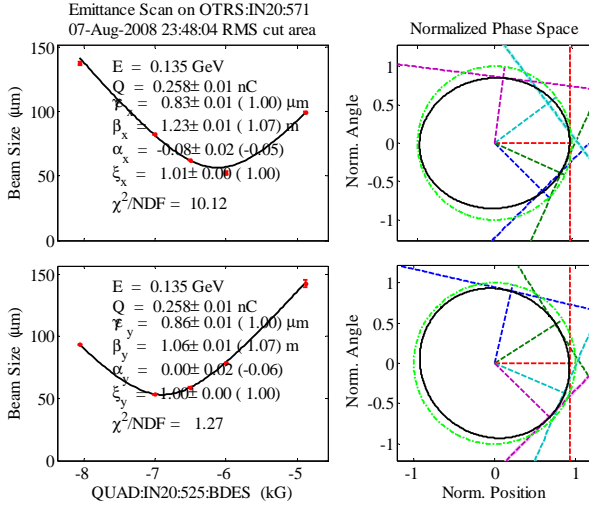


Figure 6: Emittance at OTR screen downstream of first two acceleration structures at normal operating conditions of 250 pC and 135 MeV measured by scanning an upstream quadrupole.

This procedure enables the injector to meet the performance requirements for the emittance, as can be seen in Fig. 6 for a 250 pC bunch charge. The left part shows the horizontal and vertical beam size of the central 95% of the beam distribution as a function of the quadrupole strength. The phase space ellipse from a fit to the data is on the right part and shown in units of the design ellipse at 1  $\mu\text{m}$ . The measured projected emittance is 0.85  $\mu\text{m}$  in both planes with nearly optimum match to the design ellipse.

The emittance as a function of temporal slices within the bunch can be measured in the horizontal plane by streaking the beam vertically with the transverse deflecting cavity upstream of the OTR screen. Measurements with as low a charge as 10 pC are possible on the OTR screen to measure the thermal contribution to the emittance. Figure 7 shows the horizontal slice emittance for 20 pC bunch charge and 400  $\mu\text{m}$  rms bunch length from a 0.6 mm diameter laser spot on the cathode. The emittance is almost constant at 0.14  $\mu\text{m}$  within the FWHM of the bunch. Measurements at 250 pC and 1.2 mm laser diameter give a slice emittance of 0.6  $\mu\text{m}$ .

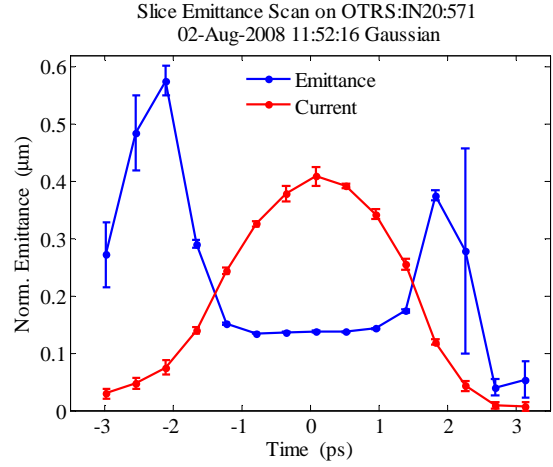


Figure 7: Slice emittance of low charge beam at 19 pC with a 0.6 mm diameter laser spot.

## BUNCH COMPRESSORS

The two 4-dipole magnetic chicane bunch compressors BC1 and BC2 in the LCLS linac are designed to compress the injector bunches from nominally 800  $\mu\text{m}$  by a factor of 4 and 10 to 200  $\mu\text{m}$  and 20  $\mu\text{m}$ , while preserving the emittance from the injector. During the first commissioning phase it was not possible to transport the chirped beam through the BC1 chicane without deterioration of the emittance from about 1  $\mu\text{m}$  to 2  $\mu\text{m}$ . This was attributed to insufficient field uniformity of the two center dipoles where the dispersed beam is about 25 mm wide. Prior to the second commissioning phase the pole width was increased and with subsequent shimming the field error could be reduced to better than 0.03% within the chirped beam width. Emittance measurements after this modification confirm that the emittance can be preserved through BC1.

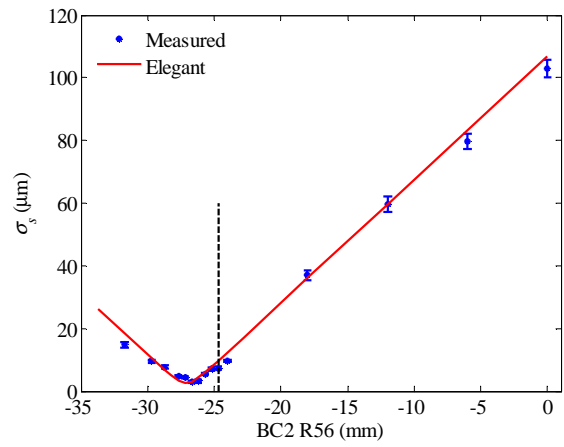


Figure 8: Bunch length after BC2 vs.  $R_{56}$  of the bunch compressor. The black line indicates the normal operating point at -24.7 mm and the red arrow the minimum bunch length.

The bunch compression and effects of coherent synchrotron radiation (CSR) on the beam were studied with both bunch compressors as a function of energy chirp from the preceding linac (BC1) or chicane  $R_{56}$  (BC2) and compared with tracking simulations [5] in Elegant [6]. The bunch length after BC1 was measured by turning off the magnets of BC2 and imposing a vertical transverse-time correlation on the bunch with the transverse cavity downstream of BC2. The beam was monitored on a phosphorescent screen in the beam switch yard downstream of L3 and the measurement calibrated by changing the transverse cavity phase while observing the vertical beam position on the screen. The bunch length after BC2 was measured in a similar way and is shown in Fig. 8 for the low charge configuration at 250 pC. The bunch length is 8  $\mu\text{m}$  at the nominal chicane  $R_{56}$  of -24.7 mm and L2 phase at -37° and has its minimum at 2  $\mu\text{m}$ . This short bunch length is at the limit of the method given by the RF-power of the transverse cavity and the resolution of the screen.

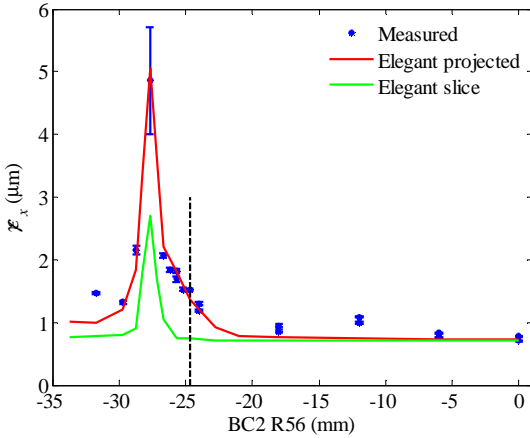


Figure 9: Horizontal normalized emittance after BC2 vs.  $R_{56}$  of the bunch compressor. The black line indicates the normal operating point at -24.7 mm.

The projected horizontal emittance as a function of BC2 chicane  $R_{56}$  was measured with the four wire scanners in L3 and is shown in Fig. 9. It illustrates the emittance growth related to the bunch compression. The large error bar of the data point at the peak in the emittance is due to the sensitivity to phase jitter at maximum compression. The simulation of the projected emittance with Elegant agrees well with the measured data and predicts in particular the doubling of the projected emittance from the value of 0.7  $\mu\text{m}$  for the straightened chicane to 1.5  $\mu\text{m}$  at the normal operating point, suggesting that the emittance growth can be entirely attributed to CSR. Although a measurement of the slice emittance which is critical for the FEL performance is not yet available downstream of the bunch compressors, a simulation of the slice emittance shows no emittance growth at the normal operating point.

## FEEDBACK SYSTEM

A number of beam based feedback systems [7] have been developed to control the most critical electron beam parameters and are based on signals from beam position monitors and coherent signals from the two bunch length monitors. The charge feedback measures the bunch charge after the gun and controls the laser power to keep the charge within 1.5% of the set point. Several independent feedback loops steer the beam after the gun, in the injector, through the X-band cavity, and into the L2 and L3 linac. The transverse beam jitter measured after BC1 is 4% of the rms beam size and 10% – 15% (see Fig. 10) near the end of the linac [8], which is near the goal of 10% set from the requirements of FEL operation.

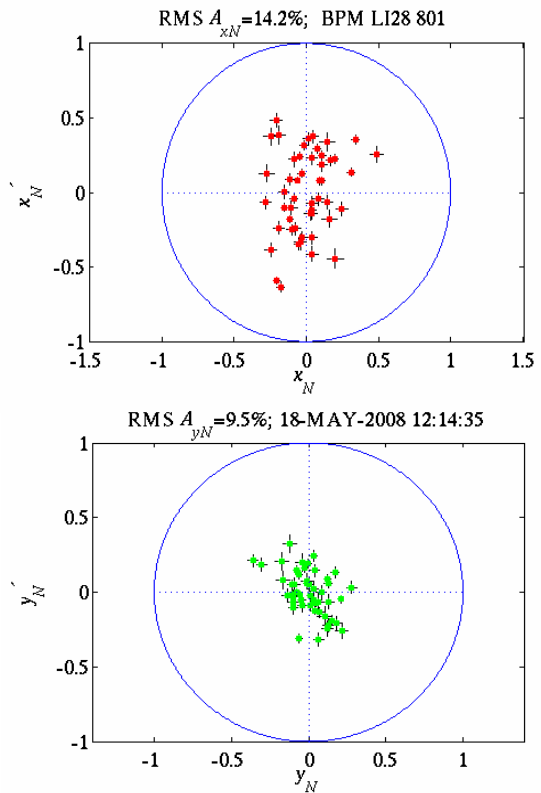


Figure 10: Shot to shot beam position and angle near the end of the linac in units normalized to the transverse beam phase space.

The feedback for the longitudinal coordinates is a combined loop for the beam energy measured with beam position monitors in DL1 and in the center of both bunch compressors as well as the bunch lengths after BC1 and BC2 measured with the relative bunch length monitors based on coherent edge radiation [9]. The feedback controls the amplitude of the L0, L1, and L2 linac for energy and the phase of L1 and L2 for bunch length. The measured energy jitter at the final energy with feedbacks in place is 0.03%. With the installation of the undulator beam line the final energy after L3 will be added to the feedback.

## ULTRA-SHORT BUNCH OPERATION

The normal operating modes of the accelerator are at 200 pC and 1 nC with bunch lengths after BC2 of 8  $\mu\text{m}$  and 20  $\mu\text{m}$  while maintaining a small emittance of 0.8  $\mu\text{m}$  and 1.2  $\mu\text{m}$ . Initial tests and simulations [10] have been done to utilize the small thermal emittance in a low-charge mode for ultra-short bunch generation. The low charge enables ultra-short bunches without adverse effects on the emittance due to CSR effects. In the experiment, a 20 pC bunch from a 4 ps FWHM laser pulse was accelerated at a -15° gun phase to a 260  $\mu\text{m}$  bunch length after the injector. The emittance of 0.2  $\mu\text{m}$  in the injector could mostly be preserved through the bunch compression with 0.2 – 0.3  $\mu\text{m}$  after BC2. Although it was not possible to measure the absolute bunch length due to insufficient measurement resolution with transverse cavity, it was likely to be about 1  $\mu\text{m}$  according to Elegant simulations. Such a short bunch length is also supported by the observation of strong near infrared COTR light at maximum compression.

## COHERENT RADIATION OBSERVATIONS

An unexpected result of the high brightness of the LCLS electron beam was the observation of coherent effects from the OTR screens along the main linac [2, 11]. The effect of this coherent optical transition radiation (COTR) is observed from the uncompressed beam after the first dogleg [12] to the compressed beam after BC2. It ranges from a small intensity enhancement of a factor 4 and about 20% changes in the beam size in the uncompressed case to an increase by a factor of up to  $10^5$  in light intensity and complex transverse distributions for highly compressed bunches.

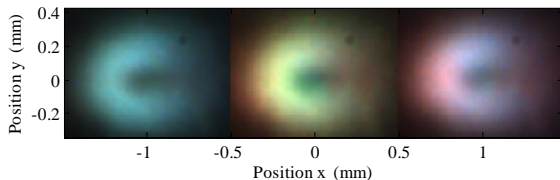


Figure 11: Coherent optical transition radiation observed with a color camera downstream of BC2.

This can be seen in Fig. 11 showing three shots of COTR images taken within one minute with a color CCD downstream of BC2. The uniformity of the spectrum within a single shot indicates transverse coherence in the micro-structure radiating at optical wavelengths. The doughnut shape is caused by destructive interference in the light emitted from the beam center [11].

## SUMMARY

The two commissioning phases of the LCLS injector and linac have succeeded in generating an electron beam

that meets all the requirements needed to operate the X-ray FEL at energies of up to 14 GeV. Figure 12 shows the projected FEL performance based on measured electron beam parameters for a period of one week. The blue curve is the simulated gain length, and saturation of the FEL is achieved for gain lengths shorter than the dashed line at 1/20th of the undulator length.

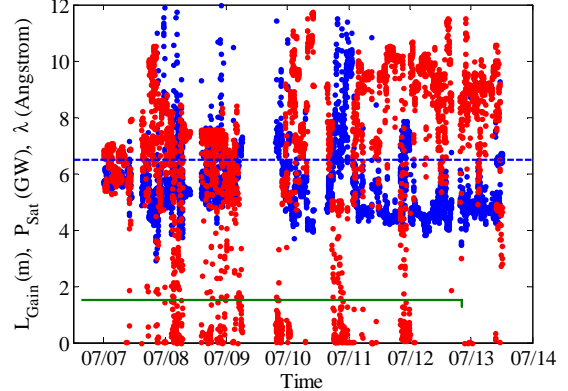


Figure 12: Simulated FEL performance based on measured electron beam parameters. The gain length is shown in blue, the saturation power in red and the wavelength in green. The dashed line represents the maximum gain length to achieve saturation.

The upcoming third phase of the LCLS commissioning starting in November 2008 will focus on the transfer line to the undulator and beginning March 2009 on the undulators with first light expected in June 2009. The installation of the laser heater in the injector is expected to mitigate the COTR effects on the OTR diagnostics and additional diagnostics to measure  $\mu\text{m}$  long bunches with spectral methods are under consideration.

## REFERENCES

- [1] J. Arthur et al., “Linac Coherent Light Source (LCLS) Conceptual Design Report”, SLAC-R-593.
- [2] R. Akre et al., Phys. Rev. ST-AB 11 (2008) 030703.
- [3] R. Akre et al., FEL’08, Gyeongju, August 2008, FRAAU04.
- [4] D. H. Dowell et al., Phys. Rev. ST-AB 9 (2006) 063502.
- [5] K.L.F. Bane et al., FEL’08, Gyeongju, August 2008, TUPPH027.
- [6] M. Borland, ANL/APS LS-287 (2000).
- [7] J. Wu et al., FEL’08, Gyeongju, August 2008, MOPPH052.
- [8] R. Akre et al., FEL’08, Gyeongju, August 2008, MOPPH051.
- [9] H. Loos et al., PAC’07, Albuquerque, August 2008, FRPMS071, p. 4191 (2007).
- [10] Y. Ding, personal communication
- [11] H. Loos et al., FEL’08, Gyeongju, August 2008, THBAU01.
- [12] D. Ratner, A. Chao, Z. Huang, FEL’08, Gyeongju, August 2008, TUPPH041.